Aalborg Universitet

Safe sub synchronous oscillations response for large DFIG-based wind farms

Fateh, Davood; Birjandi, Ali Akbar Moti; Guerrero, Josep M.

Link to publication from Aalborg University

Citation for published version (APA):
Fateh, D., Birjandi, A. A. M., & Guerrero, J. M. (2020). Safe sub synchronous oscillations response for large DFIG-based wind farms. *IEEE Access*, *8*, 169822-169834. https://doi.org/10.1109/ACCESS.2020.3019234

Safe Sub Synchronous Oscillations Response for Large DFIG-Based Wind Farms

DAVOOD FATEH[1], **ALI AKBAR MOTI BIRJANDI**[1], **(Member, IEEE),**
AND JOSEP M. GUERRERO[2], **(Fellow, IEEE)**
[1]Faculty of Electrical Engineering, Shahid Rajaee Teacher Training University, Tehran 16788-15811, Iran
[2]Center for Research on Microgrids (CROM), Department of Energy Technology, Aalborg University, 9220 Aalborg, Denmark

Corresponding author: Ali Akbar Moti Birjandi (motiebirjandi@sru.ac.ir)

ABSTRACT This paper presented an accurate analysis of the instability in DFIG-based wind farms due to the use of series compensation and provided maximum power extraction from these farms using the high compensation without the unstable sub-synchronous oscillation occurrence. For this purpose, using modal analysis, it is first shown that the main cause of this instability is low wind speed in the high compensation. This issue causes the series compensated DFIG-based wind farms is unstable due to a sub-synchronous mode. In order to prevent the unstable sub-synchronous oscillation occurrence, a supplementary controller called SSRIPC and DFIG controllers are used. Also, for good dynamic response and proper use of the SSRIPC, an objective function considered based on three factors of minimum damping ratio, overshoot, and settling time of the oscillations. By accurate optimization of the proposed controller using root-locus and PSO algorithm, it is prevented the instability caused by sub-synchronous resonance and sub-synchronous control interaction that are classes of the sub-synchronous oscillations. IEEE SSR first benchmark model and MATLAB/Simulink software are used to validate the performance of the proposed method.

INDEX TERMS Compensation level, instability, sub-synchronous oscillation, sub-synchronous resonance, sub-synchronous control interaction.

I. INTRODUCTION

Using capacitive series compensation of the line to increase the production power of the doubly-fed induction generator (DFIG) based wind farms, is more economical compared to other methods such as building the new transmission line, the network development and using the FACTS devices [1]. However, the compensation level of the transmission lines connected to the DFIG-based wind farms is not high enough, because there is the probability of the sub-synchronous oscillation (SSO) phenomenon occurrence due to the high inductive properties of the DFIGs. The SSO is a phenomenon involving coincident oscillations between two or more power system elements, such as generator–turbine, series capacitor, power electronic controllers, and HVDC controllers. The SSO is classified into three aspects: sub-synchronous resonance (SSR), sub-synchronous control interaction (SSCI), and sub-synchronous torsional interaction (SSTI).

The associate editor coordinating the review of this manuscript and approving it for publication was Derek Abbott.

It is noteworthy that, the SSR is a general issue of oscillations at the sub- synchronous frequencies. The SSR tends to involve interactions between a series compensated transmission systems and multi- mass turbine generators. It is a dynamic phenomenon with certain special characteristics and is of interest in power systems. There are two aspects of the SSR: self-excitation (SE) and torque amplification (TA).

The SE is also called the SSR in steady state. Sub-synchronous frequency currents entering the generator terminals produce sub-synchronous frequency terminal voltage components. These voltage components may sustain the currents to produce an effect that is termed the SE. The potential for the self-excitation of wind power plant (WPP), connected to a series compensated transmission line, was first reported in 2003. The two types of the SE are described as follows: induction generator effect (IGE) and Torsional interaction (TI).

Also, the TA is "transient torque" or "transient SSR". TA occurs due to faults in the network or during switching operations. This results in system disturbances.

Disturbance results in a sudden change in the current tend to cause oscillations. In a series-compensated line, oscillations that have a frequency corresponding to the resonance frequency of the network will be experienced. If the frequency of these oscillations coincides with one of the natural frequencies of the generator shaft, a large torque will be experienced. This torque is directly proportional to the magnitude of the oscillating current. SSR that is due to the TA can cause severe mechanical torsional oscillations in the shaft system that connects the generator and the turbines.

To deal with this issue, in 2005, for the first time, the Texas Public Utility Commission used the transmission line with the compensation level of 50% to transmit the wind farm power in Texas west. In addition, in the south of Minnesota, a transmission line with the compensation level of 60% was used to transfer the electrical power of a 150 MW DFIG-based wind farm. In 2009, due to the occurrence of a fault, the DFIG-based wind farm of the Texas Electric Reliability Association placed in series with a capacitive compensated transmission line and the first SSR occurred in a DFIG-based wind farm. Finally, the sub-synchronous oscillations occurred and damaged the series capacitors and the wind turbines [2]–[5]. After 2009, the studies began on a field of the SSR phenomenon and its mitigation methods in the DFIG-based wind farms. One of the SSR mitigation methods is the use of the FACTS devices. The FACTS devices can affect the resonance frequency by changing the line reactance.

In [6]–[9], the SVC was proposed to mitigate the SSR in the DFIG-based wind farms connected to a capacitive series-compensated line. In [6], one controller with a simple gain was used as the damping controller. The real power of the line is considered as the input signal to this controller. In [7] and [8], the line current was considered for the feedback signal of the SVC to damp the SSR in DFIG-based wind farms.

In [9], the impact of the TCSC was tested on the SSR. The authors in [10] and [11] used the GCSC, as the latest FACTS device to mitigate the SSR in the DFIG-based wind farms. They used a controller called the SSR damping controller (SSRDC) to control the GCSC. The use of STATCOM for the SSR mitigation in the SEIG-based wind farms is also considered in [10], [12]–[16], wherein several controllers were tested for this device. In [12], the impact of the SSSC was studied for SSR mitigation.

Despite its advantages, the use of FACTS devices and their controllers will cause the possibility of sub-synchronous control interactions (SSCI) [17]–[20]. Also, this method is costly and can produce harmonics in the system. Since the DFIG converters work similar to the FACTS devices, these converters are preferable to mitigate the SSR. In addition, there is no additional cost to use the FACTS devices. The grid side converter (GSC) of the DFIG, because of its similarity to the STATCOM, is appropriate to mitigate the SSR. For example, in [21] and [22], the reference voltages of the GSC-based wind farm were used to mitigate the SSR.

However, the results indicate that the maximum power point tracking (MPPT) is not maintained. In [23], the authors applied the rotor side converter (RSC) of DFIG to control the active power and to mitigate the SSR. Moreover, in [24], both the GSC and RSC converters were used to mitigate the SSR. But the results of these articles indicate that the MPPT is not maintained.

The author of [25] used robust nonlinear controller to damp the SSCI in DFIG-based wind farms. In [26], the series capacitor was improved for preventing the instability of the DFIG-based wind farm at the time of the SSR occurrence. Moreover, other methods have been presented to mitigate the SSR. The blocking filter (BF), which set at the natural frequency of the generator turbine shaft, was used to mitigate the torsional interaction (TI) type of the SSR [27], [28]. Nevertheless, this filter is not suitable for the SSR mitigation in the DFIG-based wind farms, because the SSR rarely occurs due to the TI in the DFIG-based wind farms. In [27]–[30], the bypass filter was used in parallel with the series capacitor of the line. This filter was set at the main frequency of the system. With this method, the current components with the frequencies lower than the main frequency pass through this filter such that the SSR does not occur. This filter is suitable to mitigate the SSR due to the induction generator effect (IGE) in the DFIG-based wind farms, because the IGE is seen in the line current oscillations. However, these filters cannot mitigate the SSR alone and quickly and are not economically suitable. Additionally, in [27], [28], [31], and [32], the sub-synchronous frequency relay and the damper winding were used to mitigate the SSR, which also are costly methods. In [33], it was declared that the SSR can be prevented by choosing the different compensation levels. This method is not suitable because selecting various compensation levels is not possible.

Also, the authors of [34]–[36] studied the SSR in the DFIG-based wind farm. In [37], a piecewise probabilistic collocation method was proposed for assessing the probabilistic stability of the SSR. As can be inferred, because of the use of capacitive series compensation for the lines connected to the DFIG-based wind farms, further studies are required in this regard.

In [38], a method with power system stabilizer presented to damp the SSR in Type-2 wind turbines. This method is good. But its results are for nominal condition (Wind speed is 12 m/s). However, it was better that this method was also tested at critical wind speed (7 m/s), because the SSR rarely occurs at high wind speed.

The author of [39] and [40] studied an analysis of the SSR in the DFIG-based wind farms. In addition, [41] presented understanding the SSO of the DFIG-based wind farms. In this reference, it is considered the wind farms without the series compensation.

The authors of [42] presented an analysis and a robust stabiliser to reduce the SSR in an IEEE FBM augmented by DFIG-based wind farm. This reference used the complex method and controller for this purpose. Also, it used the

synchronous generator in its simulation. It can help to create a good dynamic in the simulation.

This paper proposed a method using a supplementary controller called the SSR instability prevention controller (SSRIPC) to provide the high compensation level of the lines connected to the large DFIG-based wind farms at low wind speed without the unstable sub-synchronous oscillation occurrence. However, the SSRPIC can cause the SSCI instability phenomenon occurrence. This phenomenon occurs between the DFIG controllers and the supplementary controller when this controller is not set properly. For tuning the SSRPIC properly and preventing of the SSR and the SSCI, three factors to use of the SSRIPC are considered. The first factor is connection point of the SSRIPC. The SSRIPC can connect to twelve locations of the DFIG controllers. The second factor is the input signal to the SSRIPC. The voltage of the line series capacitor, the line current, and the rotor speed are candida for the input signal. The third factor is the value of SSRIPC gain. To optimize these factors, an objective function is defined based on the minimum damping ratio of the system, the overshoot of oscillations, and the settling time. PSO algorithm is used to optimize this objective function. In addition, the IEEE SSR first bench-mark model is employed to simulate in MATLAB/Simulink software.

II. SYSTEM DYNAMIC ANALYSIS

To investigate the SSR in the DFIG-based wind farms, the analysis of the small-signal stability and linearization of the system equations around the operating point are necessary. In this paper, the IEEE SSR first benchmark model is employed. This system includes a 100-MW wind farm connected to a capacitive series-compensated line. The line end is connected to the infinite bus (Fig. 1) [43]–[46]. The differential and algebraic equations of the system consist the induction generator equations, the rotor shaft equations, the transmission line equations, the RSC and the GSC controllers, and the DC-link capacitor equation between the converters. These equations are basic equations to simulate
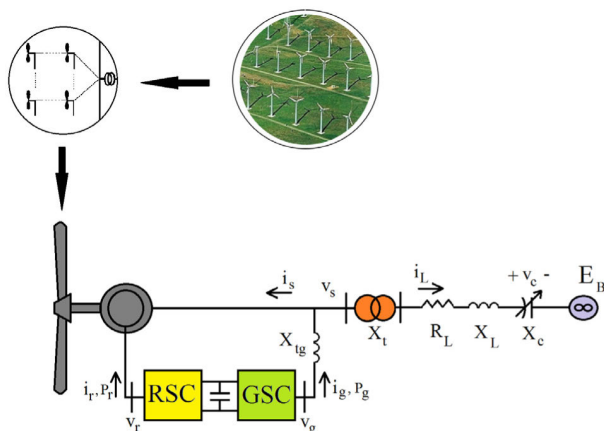

FIGURE 1. IEEE SSR first benchmark model.

in all books and articles. The state-space forms of the system equations are expressed as follows:

$$\dot{x} = f(x, u) \tag{1}$$
$$o = g(x, u) \tag{2}$$
$$\dot{y} = h(x, u) \tag{3}$$

where (1) and (2) indicate the differential equations and the algebraic equations, respectively. Also, (3) indicates the output equation. The rotor speed, the voltage of the series capacitor, and the line current can be selected as the output.

In order to analyze the SSR phenomenon and detecting the sub-synchronous mode, it is necessary to linearize the system equations around the operating point ($x = x_0$). With the linearization of these equations, (4)-(6) are obtained.

$$\Delta \dot{x} = A \cdot \Delta x + B \cdot \Delta u \tag{4}$$
$$O = F \cdot \Delta x + E \cdot \Delta u \tag{5}$$
$$\Delta Y = C \cdot \Delta x + D \cdot \Delta u \tag{6}$$

where Δx and Δu are the vectors of state variables and inputs of generators ((7) and (8)), respectively. The matrices *A, B, F, E, C,* and *D* are associated with the differential and algebraic equations.

$$\Delta x = [\Delta \psi_{qs}, \Delta \psi_{ds}, \Delta \psi_{qr}, \Delta \psi_{dr}, \Delta \omega_t, \Delta \omega_r, \ \Delta T_g, \Delta V_{DC},$$
$$\Delta I_{qL}, \Delta I_{dL}, \Delta V_{qc}, \Delta V_{dc}, \Delta i_{qr}^*, \Delta i_{dr}^*, \Delta v_{qr}, \Delta v_{dr},$$
$$\Delta i_{qg}^*, \Delta i_{dg}^*, \Delta v_{qg}, \Delta v_{dg}] \tag{7}$$
$$\Delta u = \left[\Delta i_{qs}, \Delta i_{ds}, \Delta i_{qr}, \Delta i_{dr}, \Delta v_{qs}, \Delta v_{ds}\right] \tag{8}$$

III. INDUCTION GENERATOR EQUATIONS

The induction generator has the differential and algebraic equations that are transformed into the synchronous rotating qd0-frame. Differential equations of induction generator are shown in (9)-(12) [47].

$$\dot{\psi}_{qs} = \omega_b \cdot v_{qs} - \omega_b \cdot R_s \cdot i_{qs} - \omega \cdot \psi_{ds} \tag{9}$$
$$\dot{\psi}_{ds} = \omega_b \cdot v_{ds} - \omega_b \cdot R_s \cdot i_{ds} - \omega \cdot \psi_{qs} \tag{10}$$
$$\dot{\psi}_{qr} = \omega_b \cdot v_{qr} - \omega_b \cdot R_r \cdot i_{qr} - (\omega - \omega_r) \cdot \psi_{dr} \tag{11}$$
$$\dot{\psi}_{dr} = \omega_b \cdot v_{dr} - \omega_b \cdot R_r \cdot i_{dr} - (\omega - \omega_r) \cdot \psi_{qr} \tag{12}$$

The algebraic equations of induction generators are also shown as follows [47]:

$$i_{qs} = \frac{X_{rr}}{D} \cdot \psi_{qs} - \frac{X_M}{D} \cdot \psi_{qr} \tag{13}$$
$$i_{ds} = \frac{X_{rr}}{D} \cdot \psi_{ds} - \frac{X_M}{D} \cdot \psi_{dr} \tag{14}$$
$$i_{qr} = -\frac{X_M}{D} \cdot \psi_{qs} + \frac{X_{ss}}{D} \cdot \psi_{qr} \tag{15}$$
$$i_{dr} = -\frac{X_M}{D} \cdot \psi_{ds} + \frac{X_{ss}}{D} \cdot \psi_{dr} \tag{16}$$

where ψ_{qs}, ψ_{ds}, ψ_{qr}, and ψ_{dr} are flux linkages per second of stator and rotor in the qd0-frame, respectively. The v_{qs}, v_{ds}, v_{qr}, and v_{dr} are the stator's and rotor's voltages in the qd0-frame, respectively. Also, i_{qs}, i_{ds}, i_{qr}, and i_{dr} are the stator's and rotor's currents in the qd0-frame, respectively.

The ω_b is base frequency and is equal to the synchronous frequency. Also, ω is the qd0-frame rotating speed and is equal to the base frequency in this paper. The parameters of R_s and R_r are the stator resistance and the rotor resistance, respectively. The X_{ls}, X_{lr}, and X_M are stator leakage reactance, rotor leakage reactance and magnetic reactance, respectively. Also, $X_{ss} = X_{ls} + X_M$ and $X_{rr} = X_{lr} + X_M$. All of these parameters are in the per-unit system (pu).

IV. ROTOR SHAFT EQUATIONS

In order to study SSR, wind turbine shaft is modeled with two masses. One of the masses is related to turbine shaft with low- speed and another mass is related to generator rotor shaft with high-speed. Their differential equations are shown as follows [46]:

$$\dot{\omega}_t = \frac{-D_t - D_{tg}}{2H_t} \cdot \omega_t + \frac{D_{tg}}{2H_t} \cdot \omega_r - \frac{1}{2H_t} \cdot T_g$$
$$+ \frac{1}{2H_t} \cdot T_{\text{wind}} \tag{17}$$

$$\dot{\omega}_t = \frac{D_{tg}}{2H_g} \cdot \omega_t + \frac{-D_t - D_{tg}}{2H_g} \cdot \omega_r + \frac{1}{2H_g} \cdot T_g$$
$$- \frac{1}{2H_g} \cdot T_e \tag{18}$$

$$\dot{T}_g = K_{tg} \cdot \omega \cdot \omega_t - K_{tg} \cdot \omega \cdot \omega_r \tag{19}$$

where ω_t, ω_r, and T_g are the wind turbine speed, the rotor speed, and the torque between two masses, respectively. The T_{wind} and T_e are the wind torque and the generator electrical torque, respectively. All of these parameters are in pu. D_t and D_g are the mechanical damping coefficients of the turbine and the generator, respectively. Also, H_t and H_g are the inertia constants of the turbine and the generator, respectively. The parameters of D_{tg} and K_{tg} are the damping coefficient of the shaft between the two masses and the shaft stiffness, respectively.

The electric torque is also calculated by (20). In order to obtain the MPPT, the reference electric torque is determined by a lookup table (Table 1). Based on this table, for each wind speed, the reference electric torque value is selected and applied to the RSC controller as follows:

$$T_e = 0.5X_M \cdot (i_{qs} \cdot i_{dr} - i_{ds} \cdot i_{qr}) \tag{20}$$

TABLE 1. MPPT lookup table.

$V_{\text{wind}}(m/s)$	7	8	9	10	11	12
ω_r (pu)	0.75	0.85	0.95	1.05	1.15	1.25
P_{wind} (pu)	0.32	0.49	0.69	0.95	1.25	1.6
$T_{\text{wind}} = P_{\text{wind}}/\omega_r$	0.43	0.58	0.73	0.90	1.09	1.28

V. DFIG CONVERTERS CONTROLLERS AND DC-LINK CAPACITOR

The DFIG consist of two converters that are shown in Fig. 1: the grid side converter (GSC) and the rotor side converter (RSC). The DFIG converters adjust the generator terminal

and the rotor voltages. To control these converters, the controllers shown in Figs. 2(a) and 2(b) are used. Based on the wind speed and the LOOKUP table, the reference torque is selected and applied to the RSC controller. Also, dynamics of the DC-link capacitor between the converters is modeled as a first-order equation by (21)-(23) [46].

$$C \cdot V_{\text{DC}} \cdot \frac{dV_{\text{DC}}}{dt} = -(P_r + P_g) \tag{21}$$
$$P_r = 0.5(v_{qr} \cdot i_{qr} + v_{dr} \cdot i_{dr}) \tag{22}$$
$$P_g = 0.5(v_{qg} \cdot i_{qg} + v_{dg} \cdot i_{dg}) \tag{23}$$

where P_r and P_g are the RSC and the GSC output active powers, respectively. Also, C is the DC-link capacitor. Fig. 2(c) shows the power distribution between the RSC, the GSC, and the DC-link capacitor.

The stator output reactive power is calculated by:

$$Q_s = 0.5(v_{qs} \cdot i_{ds} - v_{ds} \cdot i_{qs}) \tag{24}$$

The GSC output is connected to the generator stator output terminal by a transformer. Equations (25)-(28) represent the algebraic equations between the GSC output and the stator output terminal.

$$v_{qg} = v_{qs} + X_{tg} \cdot i_{dg} \tag{25}$$
$$v_{dg} = v_{ds} - X_{tg} \cdot i_{qg} \tag{26}$$
$$i_{qg} = i_{qs} + I_{qL} \tag{27}$$
$$i_{dg} = i_{ds} + I_{dL} \tag{28}$$

where v_{qg} and v_{dg} are the output voltage of the GSC in the qd0-frame, respectively. Also, i_{qg} and i_{dg} are the output current of the GSC in the qd0-frame, respectively. The I_{qL} and I_{dL} are the line currents in qd0-frame, respectively. The X_{tg} is the transformer impedance.

VI. DIFFERENTIAL EQUATIONS OF SERIES COMPENSATED LINE

The differential equations of the transmission line and its capacitors are presented as follows [46]:

$$\dot{I}_{qL} = -\frac{R_L}{X_L} \cdot \omega_b \cdot I_{qL} - \omega \cdot I_{dL} - \frac{\omega_b}{X_L} \cdot v_{qc} + \frac{\omega_b}{X_L} \cdot v_{qs}$$
$$- \frac{\omega_b}{X_L} \cdot E_{qB} \tag{29}$$

$$\dot{I}_{dL} = \omega \cdot I_{qL} - \frac{R_L}{X_L} \cdot \omega_b \cdot I_{dL} - \frac{\omega_b}{X_L} \cdot v_{dc} + \frac{\omega_b}{X_L} \cdot v_{ds}$$
$$- \frac{\omega_b}{X_L} \cdot E_{dB} \tag{30}$$

$$\dot{v}_{qc} = \omega_b \cdot X_c \cdot I_{qL} - \omega \cdot v_{dc} \tag{31}$$
$$\dot{v}_{dc} = \omega_b \cdot X_c \cdot I_{dL} + \omega \cdot v_{qc} \tag{32}$$

where v_{qc} and v_{dc} are the series capacitor voltages in qd0-frame, respectively. The I_{qL} and I_{dL} are the line currents in qd0-frame, respectively. Also, v_{qs}, v_{ds}, E_{qB}, and E_{dB} are the stator and the infinite bus voltages in qd0-frame, respectively. All of these parameters except ω and ω_b are in pu.
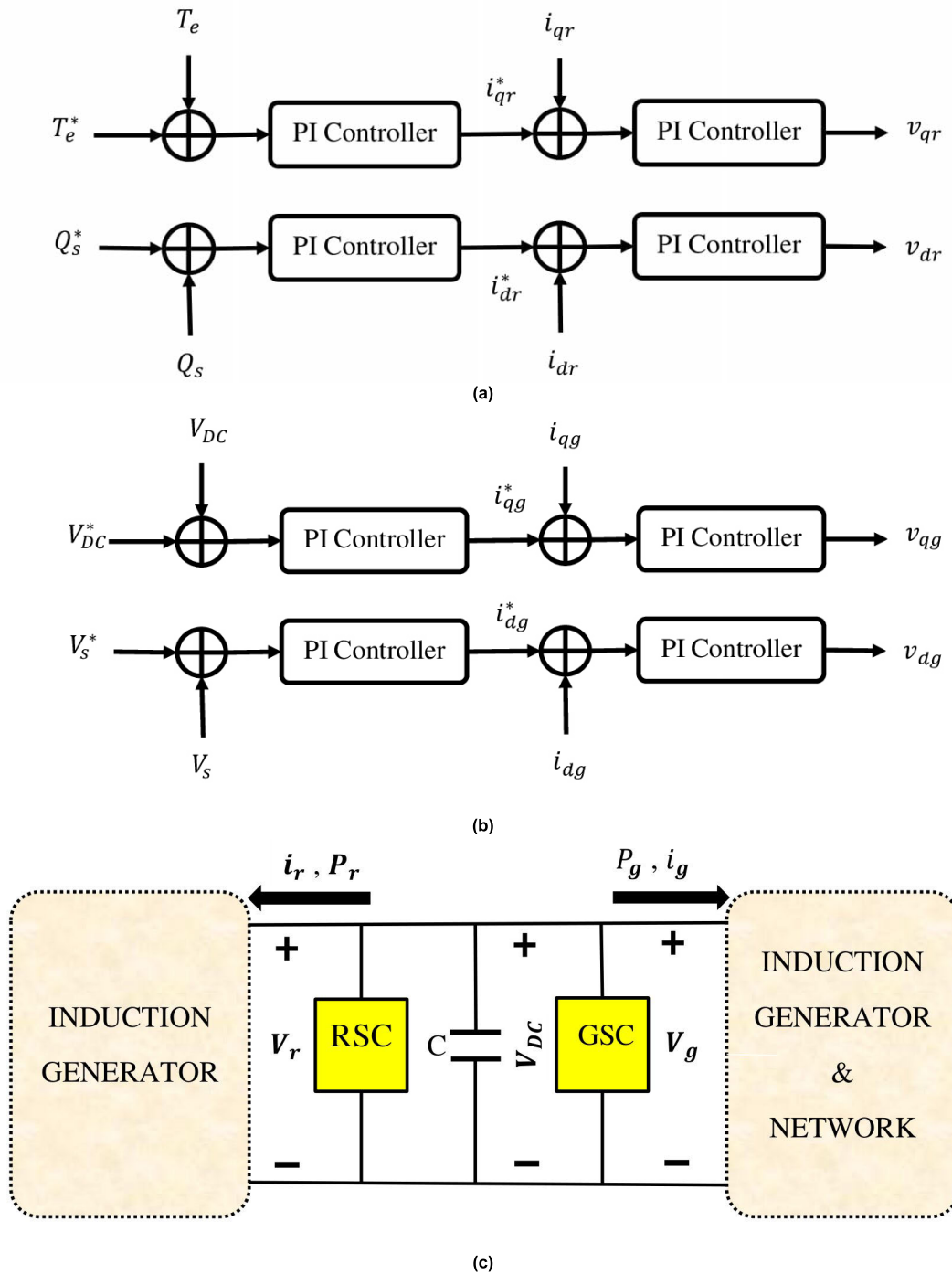
FIGURE 2. DFIG converters controllers; (a) RSC controller, (b) GSC controller, (c) power distribution between RSC, the GSC, and DC-link capacitor.

VII. SSR DEFINITON

The SSR phenomenon is the condition that the wind plant exchanges at one or more natural frequencies with the electric network. In a power system with the capacitive series compensation, the network has a natural frequency that is calculated as follows: $f_n = f_s \cdot \sqrt{X_c/X_L}$, where f_n and f_s are the natural frequency (Hz) and the synchronous frequency (Hz), respectively. Also, X_L is the line reactance (pu) and X_c is the series capacitor reactance of the line. It is the

percentage of the line reactance, which is called the compensation percentage (K %). According to f_n, slip s_n is introduced as follows [11], [46], [48]:

$$s_n = \frac{f_n - f_r}{f_n} \qquad (33)$$

where f_r is the rotor electrical frequency (Hz). As the f_n is lower than f_r, then s_n is negative. Therefore, the rotor equivalent resistor $R_{r,eq} = \frac{R_r}{s_n} < 0$ is negative in the
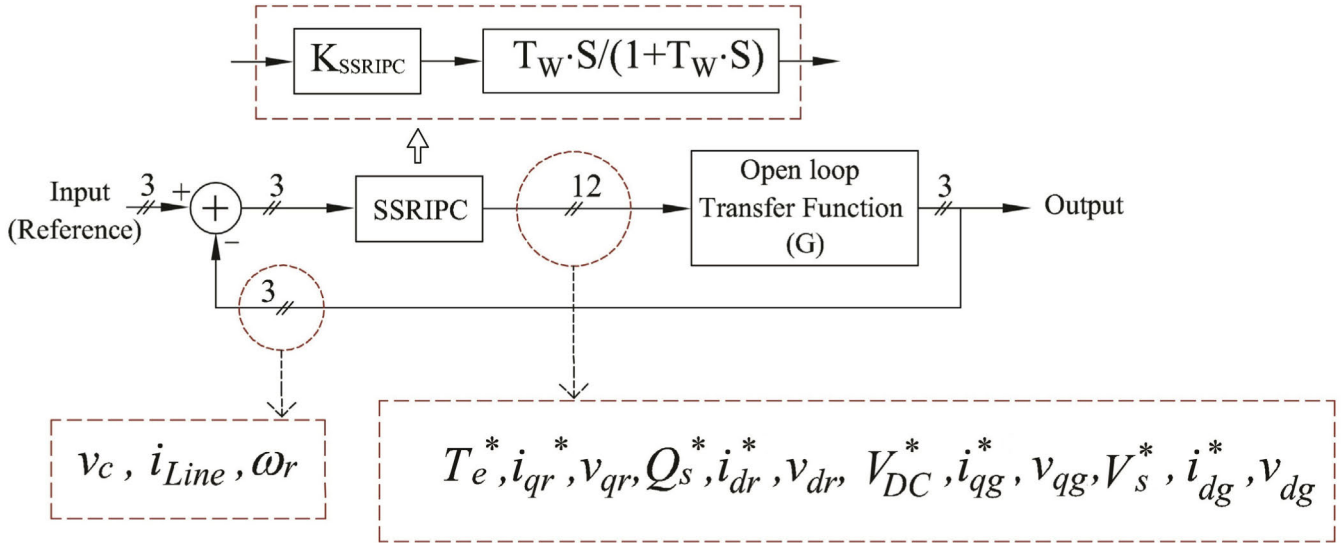
FIGURE 3. SSRIPC; signals, SSRIPC gain, and connecting location that should to optimize by PSO algorithm.

sub-synchronous frequency. If the amplitude of this resistance increases from the total resistors of the network and generator armature, then the total resistance of the system (R_{sys}) will be negative at the sub-synchronous frequency. So, according to (34), the second part of the system line current will have an exponential function with the power of positive. Therefore, the line current increases as exponentially, which this phenomenon is called the IGE. Also, due to the capacitive series compensation, a component with the resonant frequency (f_n) appears in the stator current and complementary frequency ($f_s - f_n$) of this component appears in the rotor current. If the frequency of the torsional mode between the rotor masses is close to this complementary frequency, the TI happens.

The shaft stiffness of the wind turbines is low compared to the steam, hydro and diesel generators. Also, the torsional mode of the dynamic equations of the rotor ((17)-(19)) depends greatly on the shaft stiffness (K_{tg}). For this reason, their torsional mode frequency is also low (this issue is presented in the result section). Therefore, it should be noted that the SSR in the wind power plants rarely occurs due to the TI. Because the torsional mode frequency in the wind power plants is about 1-3 Hz. Therefore, the TI occurs when the resonant frequency is between 57 to 59 Hz, which requires a very high compensation level. Thus, its probability is very low [46].

$$i = A \cdot \sin(2\pi f_s \cdot t) + e^{-(\frac{R_{sys}}{L}) \cdot t} \cdot B \cdot \sin(2\pi f_n \cdot t + \theta) \quad (34)$$

VIII. SSR INSTABILITY PREVENTION CONTROLLER
In this paper, a controller called the SSR to instability prevention controller (SSRIPC) is used to prevent the SSR instability. This controller has a gain block and a filter (washout) block [49], [50]. The DFIG's converters have eight controllers that the first, middle and end of them can be used to connect

the proposed controller. So, this controller can be connected to twelve locations of the GSC and RSC controllers. In addition, this controller needs an input signal. Since the occurred SSR is due to IGE in the DFIG-based wind farms, according to the slip s_n, the voltage of the series capacitor, the line current, and the rotor speed can be selected as the input signal to the SSRIPC, because the voltage of the series capacitor and the line current have direct effects on the IGE. Also, the rotor speed has direct effect on the rotor frequency and the slip s_n. Thus, three issues should be considered: the input signal of the SSRIPC, the value of the SSRIPC gain, and the connection point of the SSRIPC. Fig. 3 indicates the SSRIPC. In this figure, K_{SSRIPC} and T_w are the SSRIPC gain and the washout time constant, respectively. In addition, this figure shows that to use of the SSRIPC, the open loop transfer function (G) should be obtained. The input of the G is one of twelve locations to connect the SSRIPC. Also, the output of the G is one of the v_c, i_{Line}, and ω_r. To find the input signal and the connection point of the SSRIPC and to optimize the SSRIPC gain parameter, the PSO algorithm is used. This algorithm was represented by James Kendy and Rassel in 1995 [51], [52]. This algorithm is a heuristic search technique and biologically inspired by nature's social behavior of birds and fish. The algorithm is often considered under the swarm intelligence category. In this algorithm, a population move in searching for food randomly in some area. The population includes many particles. In this paper, each particle is a guess of the signal input, the value of the SSRIPC gain and the connecting location. The objective function, to prevent the SSR instability, is consists of goals: increasing the minimum damping ratio of the system in order to damp the oscillations, decreasing the overshoot in order to reduce the amplitude of oscillations and the settling time of the oscillations in order to eliminate oscillations ((35)-(38)). These three goals are considered for the good dynamic responses such as the

TABLE 2. Modes of system at wind speed of 7 M/S.

Eigenvalue number	Compensation level of 20%	Compensation level of 70%			Type of important mode
	Mode	Mode	Damping ratio	Frequency	
1	0	0	0	0	
2,3	$-976.59 \pm 4367.10i$	$-976.82 \pm 4369.9i$	0.218	695.485	
4	-2591.3	-2585.3	1	0	
5,6	$-6.2769 \pm 533.70i$	$-6.6085 \pm 639.3i$	0.01	101.7481	Super-synchronous
7,8	$-7.3310 \pm 219.56i$	$+8.4714 \pm 115.99i$	0.073	18.4607	Sub-synchronous
9	-20.0659	-20.06	1	0	
10,11	$-4.5249 \pm 96.2897.5303i$	$-22.54 \pm 96.28i$	0.228	15.3242	Electromecanical
12,13	$-0.97 \pm 6.0219i$	$-1.182 \pm 5.96i$	0.1945	0.9488	Shaft
14	-0.4382	-0.211	1	0	
15,16	$-0.0092 \pm 0.5221i$	$-0.131 \pm 0.727i$	0.1776	0.1157	
17	-0.01	-0.01	1	0	
18	-0.01	-0.01	1	0	
19	-0.0028	-0.0028	1	0	
20	-19.93	-19.93	1	0	
21	-20.79	-20.79	1	0	
22	0	0	0	0	

instability prevention, the good damping, and the low oscillation amplitude.

$$f_1 = \xi_{min} \qquad (35)$$

$$f_2 = \frac{1}{M_p} \qquad (36)$$

$$f_3 = \frac{1}{t_s} \qquad (37)$$

$$\max F = p_1 \cdot f_1 + p_2 \cdot f_2 + p_3 \cdot f_3$$

$$\sum_{j=1}^{3} p_j = 1 \qquad (38)$$

where ξ_{min} is the minimum damping ratio between all of the eigenvalues of the system. Also, M_p and t_s are the overshoot and the settling time of the oscillations, respectively. The parameters of p_1, p_2, and p_3 are the penalty factors. Here, F is the objective function.

IX. CASE STUDY AND RESULTS

In this paper, the MATLAB/Simulink software and IEEE SSR first benchmark model (Fig. 1) are used. This system has an equivalent 100-MW wind farm, which is connected to an infinite bus through a capacitive series-compensated transmission line and its parameters are given in [6] and [36]. Table 2 shows the system poles at the wind speed of 7 m/s and the compensation levels of 20% and 70%. The wind speed of 7 m/s is critical. In conditions with this wind speed, the compensation level should be less than 60% [46]. Otherwise, the SSR instability occurs. According to this table, the eigenvalues 7, 8 are the sub-synchronous mode and have the frequency of 18.4607 Hz. This mode is called the sub-synchronous mode. Also, the eigenvalues 5,6 are the super-synchronous mode and have the frequency of 101.7481 Hz. Because the stator and rotor equations are transferred to dq0-frame with the frequency of 60 Hz, so $f_s - f_n = f_{SSR}$ and the resonant frequency (f_n) is equal to

about 41.5 Hz. Since the rotor speed is 0.75 pu for the wind speed of 7 m/s, the rotor frequency is $0.75 \times 60 = 45$ Hz and the electrical mode frequency is 60-45=15 Hz. Hence, the eigenvalues 10 and 11 with the frequency 15.3242 Hz are the electromecanical mode. Its frequency is the complementary frequency (60-45=15 Hz) of electromecanical mode. The eigenvalues 12 and 13 are the shaft mode. This mode is always about 1-3 Hz in the DFIG-based wind turbines. The other modes are for other system modes and the PI controllers' modes.

Table 2 indicates that at the wind speed of 7 m/s and the compensation level of 70%, just the sub-synchronous mode is unstable. Therefore, the system at the wind speed of 7 m/s and the compensation of 70% is unstable due to the SSR. Fig. 4 shows the sub-synchronous mode at the wind speed of 7 m/s and different compensation levels. According to this figure, the compensation of 60%, exceeding which leads to instability in the system. The reason for this occurrence is that
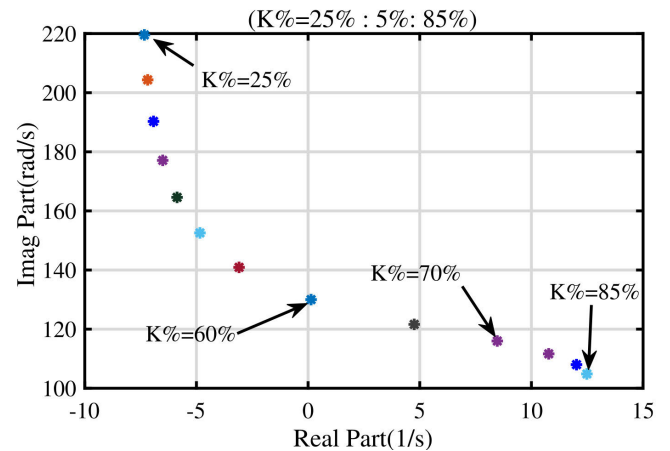

FIGURE 4. Sub-synchronous mode at wind speed of 7 m/s and different compensations levels.

increasing the compensation level causes the resonant frequency increases and the amplitude of the slip (s_n) decreases. So, the rotor's resistor amplitude increases. As the s_n and R_r/s_n are negative, the total resistor of the system will be negative and the system goes toward instability.

This paper has proposed that the SSRIPC should be connected to the v_{dg} of the GSC controller and the line series capacitor voltage should be selected for the input signal to the SSRIPC. Based on the presented method, the possibility of 70% compensation is provided without the occurrence of the instability caused by the SSR. In order to verify this proposed method, an analysis of the root-locus of the open-loop transfer function is discussed. For this purpose, the root-locus plot is sketched at the wind speed of 7 m/s and the compensation level of 70% in Fig. 5(a). Fig. 5(b) despites the root-locus near to the imag-part axis of Fig. 5(a).

The rood-locus of super-synchronous mode is shown in Fig. 6(a). Although this mode is stable, it will be unstable for $K_{critical} = 512$ and greater. In Fig. 6(b), the rood-locus of the sub-synchronous mode is presented. According to this figure, the SSR instability occurs for $K \leq 2.78$. By choosing $K > 2.78$, this mode is stable and the SSR instability does not occur. Figs. 6(c) and 6(d) show the root-locus of the shaft and electromechanical modes. These modes are stable for any amount of the K. A noteworthy point in these figures is the root-locus of one of the controllers. This mode can cause the instability for $K > 5.9$ (Fig. 6(e)). This instability is called the SSCI instability.

Hence, by choosing the K between 2.78 and 5.9, the SSR and SSCI instabilities are prevented. This range of the K is considered as a constraint for optimizing the value of the SSRIPC gain.

According to Fig. 4, to increase the line transmission power, the maximum compensation level of this system is less than 60% at the wind speed of 7 m/s without the SSR occurrence. In this paper, using the proposed controller, the maximum compensation level of the line has increased, considerably. The results of the PSO algorithm indicate the voltage of the series capacitor (v_c) is the proper input signal and the voltage of the d-axis of the GSC voltage (v_{dg}) is the proper connection point for the SSRIPC.

In addition, the optimal value of the gain (K_{SSRIPC}) is equal to 3.5. Fig. 7 shows the important poles for $K_{SSRIPC} = 3.5$ at the wind speed of 7 m/s and the compensation of 70%. Fig. 7(a) presents the super-synchronous, sub-synchronous, and electromechanical modes. In addition, Fig. 7(b) shows the PI-controller mode. According to this figure, all the modes are stable for $K = 3.5$ at the wind speed of 7 m/s and the compensation of 70%. The connection location, the gain value, and the input signal are determined once and do not change. Because they are determined using the optimization algorithm and the root-locus analysis to provide the maximum margin of stability for the system. Fig. 8 shows the sub-synchronous mode and some modes that are near to the imag-part axis. According to this figure, the SSRIPC transferred the sub-synchronous mode to a stable region. Also,
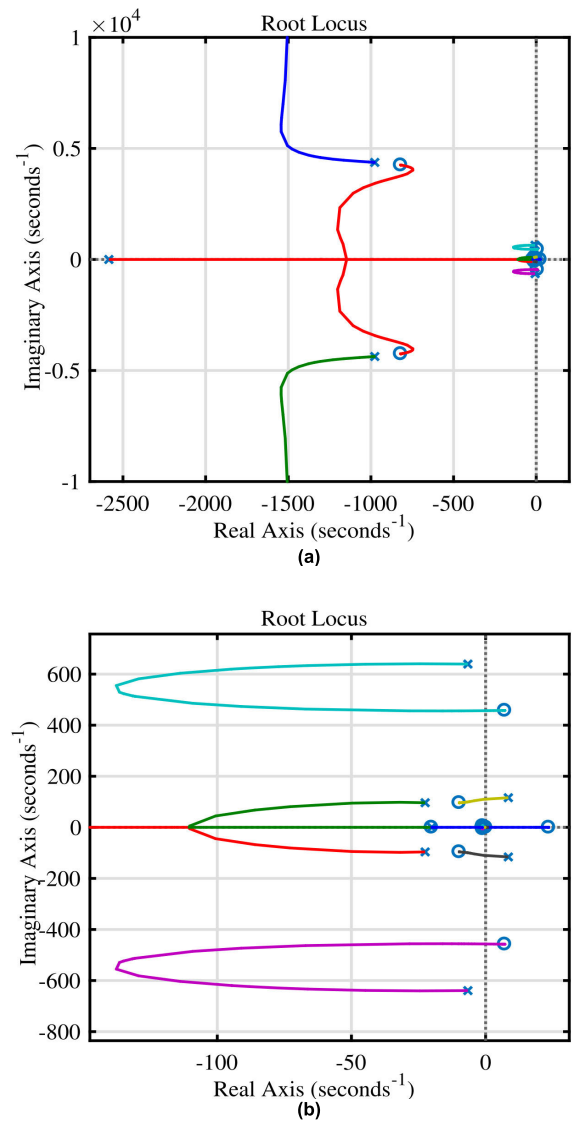

FIGURE 5. Root-locus analysis at wind speed of 7 m/s and compensation level of 70%; (a) root-locus of open-loop transfer function, (b) root-locus near to imag-part axis of Fig.5(a).

the damping ratios of other modes are better with the SSRIPC respect to without the SSRIPC.

In order to confirm the proposed method, it is initially assumed that the system has a compensation level of 20% at a wind speed of 7 m/s. Then at 100 seconds, the compensation level increases from 20% to 70%. Fig. 9(a) shows the rotor speed oscillations under the increment of the compensation level from 20% to 70%. According to this figure, because the SSR happens at the time of 100 seconds, the system without the SSRIPC is unstable. However, using the SSRIPC, the system is stable. This figure indicates that the SSRIPC creates the dynamic stability of the DFIG wind farm and permits to increase the capacitive series compensation level. Furthermore, the most important point is that the rotor speed in steady state after the increment of the compensation level
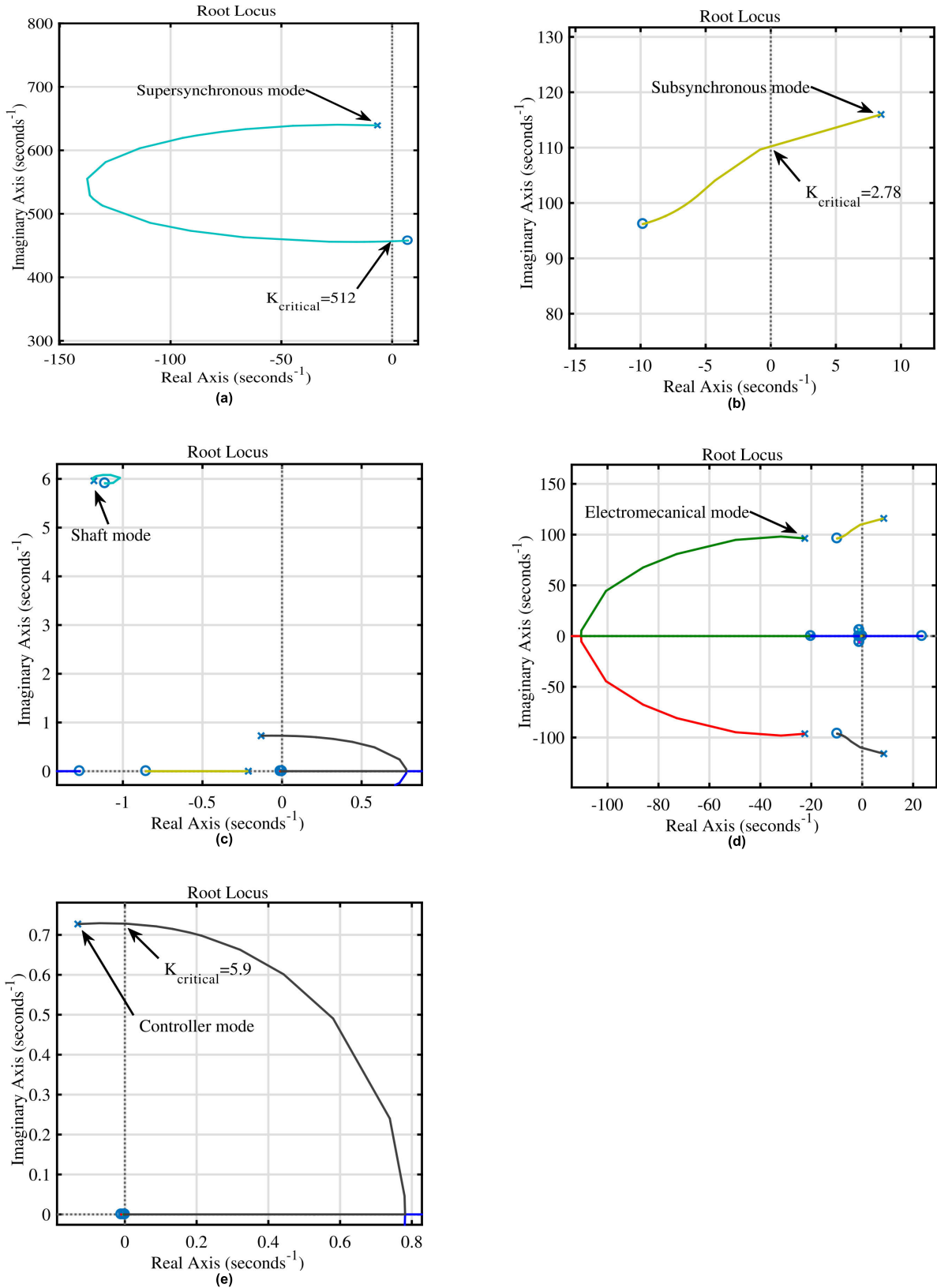
FIGURE 6. Root-locus analysis of important modes at wind speed of 7 m/s and compensation level of 70%; (a) super-synchronous mode, (b) sub-synchronous mode, (c) shaft mode, (d) electromecanical mode, (e) controller mode.
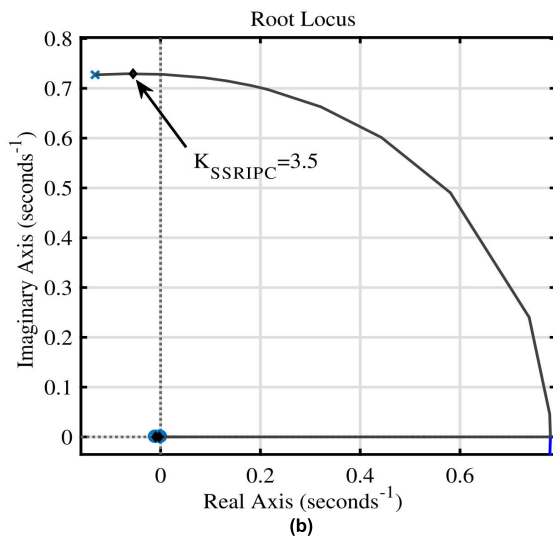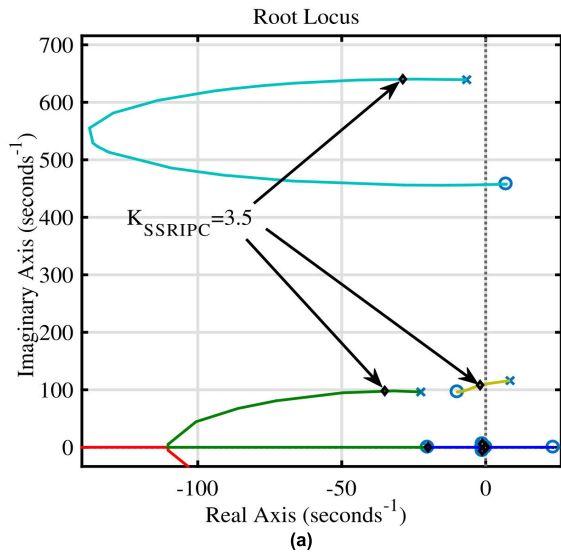
FIGURE 7. Important poles after using SSRIPC with gain of 3.5 at wind speed of 7 m/s and compensation level of 70%; (a) super-synchronous, sub-synchronous, and electromechanical modes, (b) controller mode.

FIGURE 8. System poles in cases of without SSRIPC and with SSRIPC at wind speed of 7 m/s and compensation level of 70%.

FIGURE 9. System oscillations at wind speed of 7 m/s and with increasing compensation level from 20% to 70% (Time=100s); (a) rotor speed oscillations, (b) electrical torque oscillations.

is equal to before the increase of the compensation. These results mean that the selected signal for the proposed controller and its connection point are correctly selected. The most important result is presented in Fig. 9(b), which relates to the electric torque oscillations. This figure shows very well that the SSRIPC can damp the electrical torque oscillations and also returns the electrical torque to the value before the increase in the compensation level. In other words, MPPT condition is preserved for the wind speed of 7 m/s, which is a very important. The reason for this important result is that the location to connect the SSRIPC and the input signal to it are suitable, because they did not have any direct effect on the MPPT parameters including the turbine speed, power, and torque. The SSRIPC only prevents the IGE by controlling of the line current with the help of the GSC output voltage.
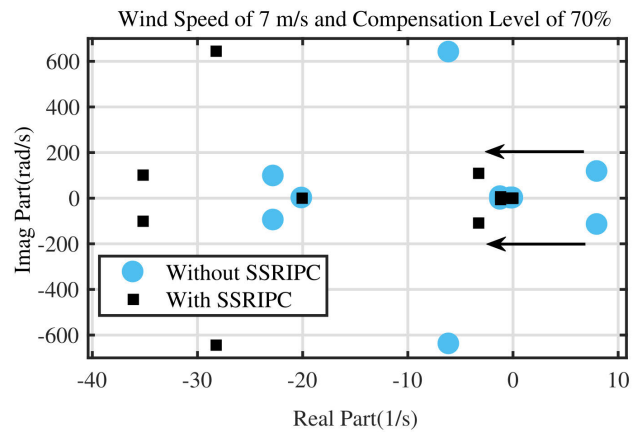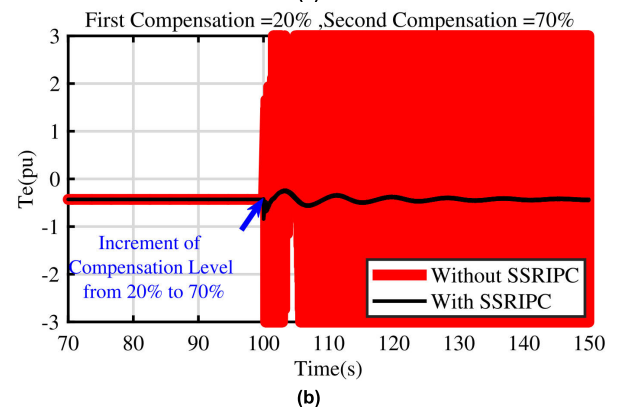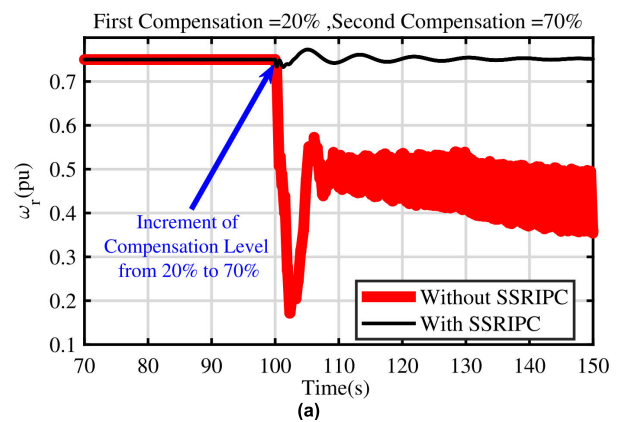
Fig. 10(a), which relates to electrical power, also confirms the maintaining of the MPPT. As stated above, the SSR in the DFIG wind farms occurs due to the IGE. Fig. 10(b) shows the increase in the line current during the SSR occurrence due to the IGE. The line current increases and oscillates under increment of the compensation level and makes the system unstable. In comparison, using the SSRIPC, the current
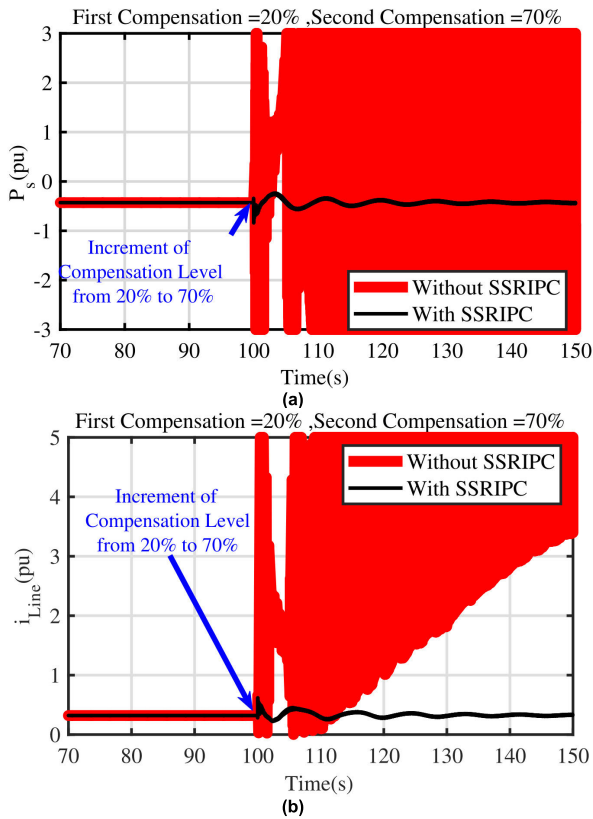
FIGURE 10. System oscillations at wind speed of 7 m/s and with increasing compensation level from 20% to 70% (Time=100s); (a) electrical power oscillations, (b) line current oscillations.

FIGURE 11. System oscillations at wind speed of 7 m/s and with increasing compensation level from 20% to 70% (Time=100s); (a) stator voltage oscillations, (b)reactive power oscillations.

oscillations damped and prevented to increase. Also, the line current returns back to the first value before the increase of the compensation. Therefore, the proposed controller is able to prevent the instability caused by the IGE using the effective factor in the sub-synchronous mode, i.e. the line series capacitor voltage.

Furthermore, Fig. 11(a) shows the stator voltage oscillations. According to this figure, by applying the proposed controller to the GSC output voltage, the stator voltage oscillations are well controlled and damped. Fig. 11(b) also shows reactive power. According to this figure, by SSRIPC, the reactive power is stable and has slight oscillations.

X. DISCUSSION

The purpose of this paper is to increase the compensation level in order to make optimal use of the power capacity of the transmission lines connected to the DFIG-based wind farms. Thus, it is necessary that the instability caused by the SSO had to be prevented. For this goal, a supplementary control was suggested in the critical condition with the critical wind speeds (7 m/s) and 70% compensation. The simulations and proposed methods of the articles in the literature are for the compensation level less than 65%. For example, in [2], the maximum compensation level was 65%, and in [22], the maximum compensation level was equal to 55%.
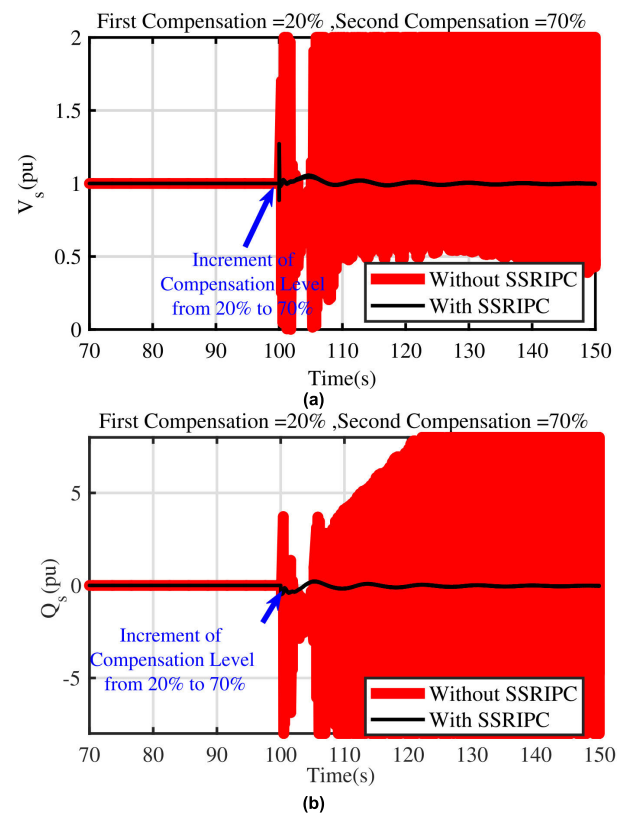
The second goal was to choose a simple and dynamic controller. For this reason, the controller was proposed with a gain and filter. The connection location of this controller and the input signal to it were also important. So, these issues were considered and the PSO algorithm was used as one of the most suitable and noteworthy algorithms. In addition, genetic algorithm (GA) has been tested which it had same results to the PSO algorithm. Further, the proposed method of this paper is simpler compared to other mitigation techniques and does not require complex mathematical methods. This paper did not used additional expensive device such as FACTS devices.

XI. CONCLUSION

The main goal and concern of this paper is to improve the power transmission capacity of lines connected to wind farms. One of the important ways to improve this issue is to use series compensation. The high compensation increases transmission capacity. On the other hand, wind speed is fluctuating at wind farm sites. The low wind speeds and the high compensation levels create exacerbated instability. Therefore, the main concern of this paper is to improve the transmission power with the help of high compensation at very low and critical wind speeds. For this purpose, this paper studied and prevented the SSO phenomenon occurrence in the series

compensated large DFIG-based wind farms using a supplementary controller called the SSR instability prevention controller (SSRIPC). The root-locus analysis is performed to show the elements, which are effective in the SSO. According to this analysis, it is found that the sub-synchronous mode and the controller mode are mainly responsible for exposing the DFIG-based wind farms to the SSO occurrence. However, the SSO does not occur in the DFIG-based wind farms, if the SSRIPC parameters, the input signal to it and its connection point are properly selected. For this purpose, the PSO algorithm is used to optimize three factors: the input signal to the SSRIPC, the gain of the SSRIPC, and the connection point of the SSRIPC. According to the PSO results, the d-axis of GSC output voltage is the best location to connect the SSRIPC and the series capacitor voltage is the best input signal for the SSRIPC. To investigate the performance of the proposed method, the IEEE SSR first bench-mark model was simulated using the dynamic equations in the MATLAB/Simulink and applied the proposed method on it. The simulation results indicate that the proposed method is accurate and very effective. As, the SSR instability is prevented at the high compensation level and the low wind speed. Furthermore, this method enhances the damping of the oscillations and reduces their amplitude. On the order hand, the use of this method does not change the MPPT conditions. Also, this method is simpler compared to other mitigation techniques and does not require complex mathematical methods.

REFERENCES

[1] *Series Compensation, Boosting Transmission Capacity*. [Online]. Available: http://www.abb.com/FACTS

[2] H. A. Mohammadpour and E. Santi, "Optimal adaptive sub-synchronous resonance damping controller for a series-compensated doubly-fed induction generator-based wind farm," *IET Renew. Power Gener.*, vol. 9, no. 6, pp. 669–681, Aug. 2015.

[3] M. Sahni, Y. Cheng, and Y. Zhou, "Sub-synchronous interaction in wind power Plants–Part II: An ercot case study," in *Proc. IEEE Power Energy Soc. Gen. Meeting*, San Diego, CA, USA, Jul. 2012, pp. 1–9, doi: 10.1109/PESGM.2012.6345355.

[4] M. Sahni, D. Muthumuni, B. Badrzadeh, A. Gole, and A. Kulkarni, "Advanced screening techniques for sub-synchronous interaction in wind farms," in *Proc. PES T&D*, Orlando, FL, USA, May 2012, pp. 1–9, doi: 10.1109/TDC.2012.6281671.

[5] L. Wang, X. Xie, Q. Jiang, and H. R. Pota, "Mitigation of multimodal subsynchronous resonance via controlled injection of supersynchronous and subsynchronous currents," *IEEE Trans. Power Syst.*, vol. 29, no. 3, pp. 1335–1344, May 2014.

[6] H. Xie and M. M. de Oliveira, "Mitigation of SSR in presence of wind power and series compensation by SVC," in *Proc. Int. Conf. Power Syst. Technol.*, Chengdu, China, Oct. 2014, pp. 2819–2826, doi: 10.1109/POWERCON.2014.6993811.

[7] D. H. R. Suriyaarachchi, U. D. Annakkage, C. Karawita, D. Kell, R. Mendis, and R. Chopra, "Application of an SVC to damp subsynchronous interaction between wind farms and series compensated transmission lines," in *Proc. IEEE Power Energy Soc. Gen. Meeting*, San Diego, CA, USA, Jul. 2012, pp. 1–6, doi: 10.1109/PESGM.2012.6344797.

[8] B. V P, M. Ahamed R, K. Devi R P, and R. R, "Analysis and mitigation of subsynchronous oscillations in a radially-connected wind farm," in *Proc. Power Energy Syst., Towards Sustain. Energy*, Bengaluru, India, Mar. 2014, pp. 1–7, doi: 10.1109/PESTSE.2014.6805280.

[9] R. K. Varma, S. Auddy, and Y. Semsedini, "Mitigation of subsynchronous resonance in a series-compensated wind farm using FACTS controllers," *IEEE Trans. Power Del.*, vol. 23, no. 3, pp. 1645–1654, Jul. 2008.

[10] H. A. Mohammadpour and E. Santi, "Modeling and control of gate-controlled series capacitor interfaced with a DFIG-based wind farm," *IEEE Trans. Ind. Electron.*, vol. 62, no. 2, pp. 1022–1033, Feb. 2015.

[11] H. A. Mohammadpour, Y.-J. Shin, and E. Santi, "SSR analysis of a DFIG-based wind farm interfaced with a gate-controlled series capacitor," in *Proc. IEEE Appl. Power Electron. Conf. Expo. (APEC)*, Fort Worth, TX, USA, Mar. 2014, pp. 3110–3117, doi: 10.1109/APEC.2014.6803749.

[12] M. S. El Moursi and V. Khadkikar, "Novel control strategies for SSR mitigation and damping power system oscillations in a series compensated wind park," in *Proc. 38th Annu. Conf. IEEE Ind. Electron. Soc. (IECON)*, Montreal, QC, Canada, Oct. 2012, pp. 5335–5342, doi: 10.1109/IECON.2012.6389534.

[13] S. Golshannavaz, M. Mokhtari, and D. Nazarpour, "SSR suppression via STATCOM in series compensated wind farm integrations," in *Proc. 19th Iranian Conf. Elect. Eng.*, Tehran, Iran, May 2011, pp. 1–6.

[14] A. F. Abdou, A. Abu-Siada, and H. R. Pota, "Damping of subsynchronous oscillations and improve transient stability for wind farms," in *Proc. IEEE PES Innov. Smart Grid Technol.*, Perth, WA, Ausralia, Nov. 2011, pp. 1–6, doi: 10.1109/ISGT-Asia.2011.6167077.

[15] A. Moharana, R. K. Varma, and R. Seethapathy, "SSR mitigation in wind farm connected to series compensated transmission line using STATCOM," in *Proc. IEEE Power Electron. Mach. Wind Appl.*, Denver, CO, USA, Jul. 2012, pp. 1–8, doi: 10.1109/PEMWA.2012.6316401.

[16] A. Moharana, R. K. Varma, and R. Seethapathy, "SSR alleviation by STATCOM in Induction-Generator-Based wind farm connected to series compensated line," *IEEE Trans. Sustain. Energy*, vol. 5, no. 3, pp. 947–957, Jul. 2014.

[17] X. Zhang, X. Xie, H. Liu, H. Liu, Y. Li, and C. Zhang, "Mitigation of subsynchronous control interaction in wind power systems with GA-SA tuned damping controller," *IFAC-PapersOnLine*, vol. 50, no. 1, pp. 8740–8745, Jul. 2017.

[18] Y. Wang, "H∞ current damping control of DFIG based wind farm for sub-synchronous control interaction mitigation," *Int. J. Elect. Power Energy Syst.*, vol. 98, pp. 509–519, Jun. 2018.

[19] H. Liu, X. Xie, Y. Li, H. Liu, and Y. Hu, "Mitigation of SSR by embedding subsynchronous notch filters into DFIG converter controllers," *IET Gener., Transmiss. Distrib.*, vol. 11, no. 11, pp. 2888–2896, Aug. 2017.

[20] H. Liu, X. Xie, C. Zhang, Y. Li, H. Liu, and Y. Hu, "Quantitative SSR analysis of series-compensated DFIG-based wind farms using aggregated RLC circuit model," *IEEE Trans. Power Syst.*, vol. 32, no. 1, pp. 474–483, Jan. 2017.

[21] L. Fan and Z. Miao, "Mitigating SSR using DFIG-based wind generation," *IEEE Trans. Sustain. Energy*, vol. 3, no. 3, pp. 349–358, Jul. 2012.

[22] H. A. Mohammadpour, A. Ghaderi, H. Mohammadpour, and E. Santi, "SSR damping in wind farms using observed-state feedback control of DFIG converters," *Electr. Power Syst. Res.*, vol. 123, pp. 57–66, Jun. 2015.

[23] Z. Bin, L. Hui, W. Mingyu, C. Yaojun, L. Shengquan, Y. Dong, Y. Chao, H. Yaogang, and C. Zhe, "An active power control strategy for a DFIG-based wind farm to depress the subsynchronous resonance of a power system," *Int. J. Electr. Power Energy Syst.*, vol. 69, pp. 327–334, Jul. 2015.

[24] H. A. Mohammadpour and E. Santi, "SSR damping controller design and optimal placement in rotor-side and grid-side converters of series-compensated DFIG-based wind farm," *IEEE Trans. Sustain. Energy*, vol. 6, no. 2, pp. 388–399, Apr. 2015.

[25] P. Li, J. Wang, L. Xiong, and M. Ma, "Robust nonlinear controller design for damping of sub-synchronous control interaction in DFIG-based wind farms," *IEEE Access*, vol. 7, pp. 16626–16637, Jan. 2019.

[26] H. Xie, M. Monge, B. Li, C. Heyman, and M. M. de Oliveira, "Subsynchronous resonance characteristics in presence of doubly-fed induction generator and series compensation and mitigation of subsynchronous resonance by proper control of series capacitor," *IET Renew. Power Gener.*, vol. 8, no. 4, pp. 411–421, May 2014.

[27] K. R. Padiyar, *Power System Dynamics Stability and Control*. Hyderabad, India: BS Publications, 2011.

[28] K. R. Padiyar, *Analysis of Subsynchronous Resonance in Power System*. Boston, MA, USA: Kluwer, 1999.

[29] G. D. Irwin, A. K. Jindal, and A. L. Isaacs, "Sub-synchronous control interactions between type 3 wind turbines and series compensated AC transmission systems," in *Proc. IEEE Power Energy Soc. Gen. Meeting*, Jul. 2011, pp. 1–6, doi: 10.1109/PES.2011.6039426.

[30] J. D. S. Han, "ERCOT CREZ reactive power compensation study," Tech. Rep., 2010.

[31] K. Narendra, "New microprocessor based relay to monitor and protect power systems against sub-harmonics," in *Proc. IEEE Elect. Power Energy Conf.*, Winnipeg, MB, Canada, Oct. 2011, pp. 438–443, doi: 10.1109/EPEC.2011.6070241.

[32] "Reader's guide to subsynchronous resonance," *IEEE Trans. Power Syst.*, vol. 7, no. 1, pp. 150–157, Feb. 1992.

[33] M. Bongiorno and A. Petersson, "The impact of wind farms on subsynchronous resonance in power systems-elforsk," Rapport, Tech. Rep., 2011, vol. 11, p. 29.

[34] X. Xie, X. Zhang, H. Liu, H. Liu, Y. Li, and C. Zhang, "Characteristic analysis of subsynchronous resonance in practical wind farms connected to series-compensated transmissions," *IEEE Trans. Energy Convers.*, vol. 32, no. 3, pp. 1117–1126, Sep. 2017.

[35] Y. Song and F. Blaabjerg, "Overview of DFIG-based wind power system resonances under weak networks," *IEEE Trans. Power Electron.*, vol. 32, no. 6, pp. 4370–4394, Jun. 2017.

[36] Y. Song, X. Wang, and F. Blaabjerg, "Impedance-based high-frequency resonance analysis of DFIG system in weak grids," *IEEE Trans. Power Electron.*, vol. 32, no. 5, pp. 3536–3548, May 2017.

[37] W. Chen, X. Xie, D. Wang, H. Liu, and H. Liu, "Probabilistic stability analysis of subsynchronous resonance for series-compensated DFIG-based wind farms," *IEEE Trans. Sustain. Energy*, vol. 9, no. 1, pp. 400–409, Jan. 2018.

[38] F. Mancilla-David, "Modeling and control of type-2 wind turbines for sub-synchronous resonance damping," *Energy Convers. Manage.*, vol. 97, pp. 315–322, Jun. 2015.

[39] K. Gu, "SSR analysis of DFIG-based wind farm with VSM control strategy," *IEEE Access*, vol. 7, pp. 118702–118711, 2019.

[40] X. Zhang, "Impedance modeling and SSR analysis of DFIG using complex vector theory," *IEEE Access*, vol. 7, pp. 155860–155870, Oct. 2019.

[41] Y. Xu, "Understanding subsynchronous oscillations in DFIG-based wind farms without series compensation," *IEEE Access*, vol. 7, pp. 107201–107210, 2019.

[42] N. N. Shah and S. R. Joshi, "Analysis, reduction and robust stabiliser design of sub-synchronous resonance in an IEEE FBM augmented by DFIG-based wind farm," *IET Renew. Power Gener.*, vol. 13, no. 16, pp. 3151–3167, Dec. 2019.

[43] N. W. Miller, J. J. Sanchez-Gasca, W. W. Price, and R. W. Delmerico, "Dynamic modeling of GE 1.5 and 3.6 MW wind turbine-generators for stability simulations," in *Proc. IEEE Power Eng. Soc. Gen. Meeting*, Toronto, Ont., Canada, Jul. 2003, pp. 1977–1983, doi: 10.1109/PES.2003.1267470.

[44] J. T. Bialasiewicz and E. Muljadi, "The wind farm aggregation impact on power quality," in *Proc. 32nd Annu. Conf. IEEE Ind. Electron. (IECON)*, Paris, France, Nov. 2006, pp. 4195–4200, doi: 10.1109/IECON.2006.347614.

[45] L. M. Fernández, F. Jurado, and J. R. Saenz, "Aggregated dynamic model for wind farms with doubly fed induction generator wind turbines," *Renew. Energy*, vol. 33, no. 1, pp. 129–140, Jan. 2008.

[46] L. Fan, R. Kavasseri, Z. L. Miao, and C. Zhu, "Modeling of DFIG-based wind farms for SSR analysis," *IEEE Trans. Power Del.*, vol. 25, no. 4, pp. 2073–2082, Oct. 2010.

[47] P. C. Krause, O. Wasynczuk, and S. D. Sudhoff, *Analysis of Electric Machinery*. New York, NY, USA: IEEE Press, 1995.

[48] L. Fan, C. Zhu, Z. Miao, and M. Hu, "Modal analysis of a DFIG-based wind farm interfaced with a series compensated network," *IEEE Trans. Energy Convers.*, vol. 26, no. 4, pp. 1010–1020, Dec. 2011.

[49] P. Kundur, *Power System Stability and Control*. New York, NY, USA: McGraw-Hill, 1994.

[50] A. A. Motiebirjandi and D. Fateh, "Optimal placement method of multi UPFCs to damp power system oscillations," *Int. Trans. Electr. Energy Syst.*, vol. 27, no. 9, p. e2360, May 2017.

[51] R. Eberhart and J. Kennedy, "A new optimizer using particle swarm theory," in *Proc. 6th Int. Symp. Micro Mach. Hum. Sci.*, Nagoya, Japan, Oct. 1995, pp. 39–43, doi: 10.1109/MHS.1995.494215.

[52] J. Kennedy and R. Eberhart, "Particle swarm optimization," in *Proc. Int. Conf. Neural Netw. (ICNN)*, Perth, WA, Australia, Nov./Dec. 1995, pp. 1942–1948, doi: 10.1109/ICNN.1995.488968.

DAVOOD FATEH received the B.Sc. degree in electrical power engineering from Islamic Azad University, Saveh, Iran, in 2010, and the M.Sc. degree in electrical power engineering from Shahid Rajaee Teacher Training University (SRTTU), Tehran, Iran, in 2013, where he is currently pursuing the Ph.D. degree with the Faculty of Electrical Engineering. His research interests include power systems, dynamic stability of power systems, and dynamic analysis of DFIG-based wind farms.

ALI AKBAR MOTI BIRJANDI (Member, IEEE) received the B.Sc. degree in electronic engineering from the Babol Noshirvani University of Technology, Babol, Iran, in 1991, the M.Sc. degree in electrical engineering from the Iran University of Science and Amp Technology, Tehran, Iran, in 1994, and the Ph.D. degree in electrical engineering from the Moscow Power Engineering Institute (Technical University), in 2004. He is currently an Associate Professor with the Department of Electrical Engineering, Shahid Rajaee Teacher Training University, Iran. His research interests include design and control of microgrid, distributed generation, dc–dc converter for renewable energy source, power electronics application for flexible AC transmission systems (FACTS), power quality, and renewable energy systems and amp applications. He is a member of the Iranian Power Electronics Society (PESI).

JOSEP M. GUERRERO (Fellow, IEEE) received the B.S. degree in telecommunications engineering, the M.S. degree in electronics engineering, and the Ph.D. degree in power electronics from the Technical University of Catalonia, Barcelona, in 1997, 2000, and 2003, respectively.

Since 2011, he has been a Full Professor with the Department of Energy Technology, Aalborg University, Denmark. In 2014, he was a Chair Professor with Shandong University. In 2015, he was a Distinguished Guest Professor with Hunan University. In 2016, he was a Visiting Professor Fellow with Aston University, U.K., and a Guest Professor with the Nanjing University of Posts and Telecommunications. In 2019, he was also a Villum Investigator with the Villum Fonden, Center for Research on Microgrids (CROM), Aalborg University, where he was the Founder and the Director. He is currently with the Microgrid Research Program, Aalborg University. He has published more than 600 journal articles in microgrids and renewable energy systems, which are cited more than 50,000 times. His contributions are on distributed power systems and microgrids, in 2015. His research interests include oriented to different microgrid aspects, including power electronics, distributed energy-storage systems, hierarchical and cooperative control, energy management systems, smart metering, the Internet of Things for AC/DC microgrid clusters, islanded minigrids, microgrid technologies applied to offshore wind, maritime microgrids for electrical ships, vessels, ferries, and seaports, and space microgrids applied to nanosatellites and spacecrafts. He received the Best Paper Award from the IEEE TRANSACTIONS ON ENERGY CONVERSION from 2014 to 2015, the Best Paper Prize from the IEEE-PES in 2015, and the Best Paper Award from the *Journal of Power Electronics* in 2016. During six consecutive years, from 2014 to 2019, he was awarded from Clarivate Analytics (Thomson Reuters) as Highly Cited Researcher with 50 highly cited articles. He serves as an Associate Editor for a number of the IEEE TRANSACTIONS.

• • •